Supplementary Material for

Bubble motion in a vertical capillary with an external flow

Yingxian Estella Yu,[1] Mirco Magnini,[2] Lailai Zhu,[1,3] Suin Shim,[1] and Howard A. Stone[1,*]

[1]*Department of Mechanical and Aerospace Engineering, Princeton University, Princeton, NJ 08544, USA*

[2]*Department of Mechanical, Materials and Manufacturing Engineering, University of Nottingham, Nottingham, NG7 2RD, UK*

[3]*Department of Mechanical Engineering, National University of Singapore, 117575, Singapore*

(Dated: October 15, 2020)

I. TIME-DEPENDENT DYNAMICS OF ASYMMETRIC BUBBLES

We investigate the transition process of a bubble from a steady-state axisymmetric profile to an asymmetric profile, resulting from a sudden change in the downward liquid flow rate (i.e., Ca_l), which forces the bubble to transition from one solution branch to another. We consider the case at $\mathrm{Bo} = 1.56$ in detail, with the two axisymmetric film thickness solution branches documented in Fig. 4(e),(f) and Fig. 5 of the manuscript. When moving along the right solution branch towards the left, the theoretical model suggests that the branch should terminate before $\mathrm{Ca}_l = -0.005$ is achieved. When moving along the left branch towards the right, on the other hand, the theoretical model yields solutions up to $\mathrm{Ca}_l = 0$. The overlapping domain of the two solution branches not only yields hysteresis in the axisymmetric film thickness, as is documented in the manuscript, but symmetry-breaking in the bubble profile is also observed as the film thickness solution attempts to transition from one branch to the other.

Numerical simulations on the right solution branch are run starting from $\mathrm{Ca}_l = 0.01$. The bubble profile on this solution branch is characterized by a thick annular film, with the bubble "nose" (which smoothly connects to the uniform film region) pointing upward, and the "tail" (with connects to the uniform film region with undulations) appearing at the bottom end of the bubble. The external background flow characterized by Ca_l is gradually reduced in order to move along the right solution branch towards the left, and the simulation is run until the steady state is achieved before Ca_l is further reduced. On this branch, the smallest Ca_l that yields steady-state axisymmetric dynamics is $\mathrm{Ca}_l = -0.003$. A further decrease of the liquid flow rate to $\mathrm{Ca}_l = -0.004$ yields a transition to an asymmetric bubble dynamics as documented in detail in Section 4.2.2 of the manuscript.

On the left branch, numerical simulations are run starting from $\mathrm{Ca}_l = -0.02$. The solution on this branch is characterized by a thin annular film, with the "nose" pointing downward and the "tail" appearing at the top end of the bubble. The external flow Ca_l is gradually increased to move along the solution branch towards the right, each time until steady state. The results of two-dimensional axisymmetric simulations and three-dimensional simulations match exactly on this branch until $\mathrm{Ca}_l = -0.004$. However, when the liquid flow rate is further increased to $\mathrm{Ca}_l = -0.003$ and above, the three-dimensional simulation transitions

* hastone@princeton.edu.

to the asymmetric dynamics, whereas the results of the axisymmetric simulations achieve steady conditions that stay on the left branch and agree well with the theory. This asymmetric bubble dynamics is described in detail in Section II below.

II. TRANSITION FROM THE LEFT SOLUTION BRANCH TO THE RIGHT BRANCH: FROM $\mathbf{Ca}_l = -0.004$ TO $\mathbf{Ca}_l = -0.003$

In this section, we describe the time-dependent dynamics of a bubble that begins with an axisymmetric steady-state solution located at $\mathrm{Ca}_l = -0.004$ on the left solution branch, obtained from a three-dimensional simulation by slowly increasing Ca_l from -0.02. This data point is located on the left solution branch in Fig. 4(e) of the manuscript. At $t = 0$, the bubble is sinking steadily and axisymmetrically with its "nose" pointing downward, with $\mathrm{Ca}_b = -0.00415$ and a very thin film $b/R = 0.0214$. This steady bubble shape is shown in Fig. 1(a) at $t/\tau = 0$, and these steady conditions are now used as the initial conditions for a new simulation where Ca_l is increased to $\mathrm{Ca}_l = -0.003$. When $t > 0$, the bubble transitions across three different unsteady regimes as time elapses, which are described in detail in the subsections below, with the aid of Fig. 1.

Note that when reaching $\mathrm{Ca}_l = -0.003$ from the right branch, which is the initial condition shown in Section 4.2.2 of the manuscript, the three-dimensional simulation achieves a steady-state axisymmetric solution with the bubble sinking with "nose" pointing upward.

A. Stage 1: (Almost) Symmetric adjustment to $\mathbf{Ca}_l = -0.003$

During stage 1, a film thinning wave is generated from the "nose" (bottom end) of the bubble, which travels upward and generates a thinner film. The initial stage lasts until $t/\tau \approx 4$, and a bubble profile during this stage can be seen in Fig. 1(a) at $t/\tau = 1.2$. During this process, the wave thins the film down to $b/R = 0.0175$, and the bubble "nose" and "tail" travel steadily at $\mathrm{Ca}_b = -0.00309$, see Fig. 1(a); these values agree well with the steady-state results of a two-dimensional axisymmetric simulation at $\mathrm{Ca}_l = -0.003$ run with the same initial conditions, which eventually yields an axisymmetric steady solution on the left branch.

Although the film thickness at stage 1 seems to converge to a steady-state axisymmetric

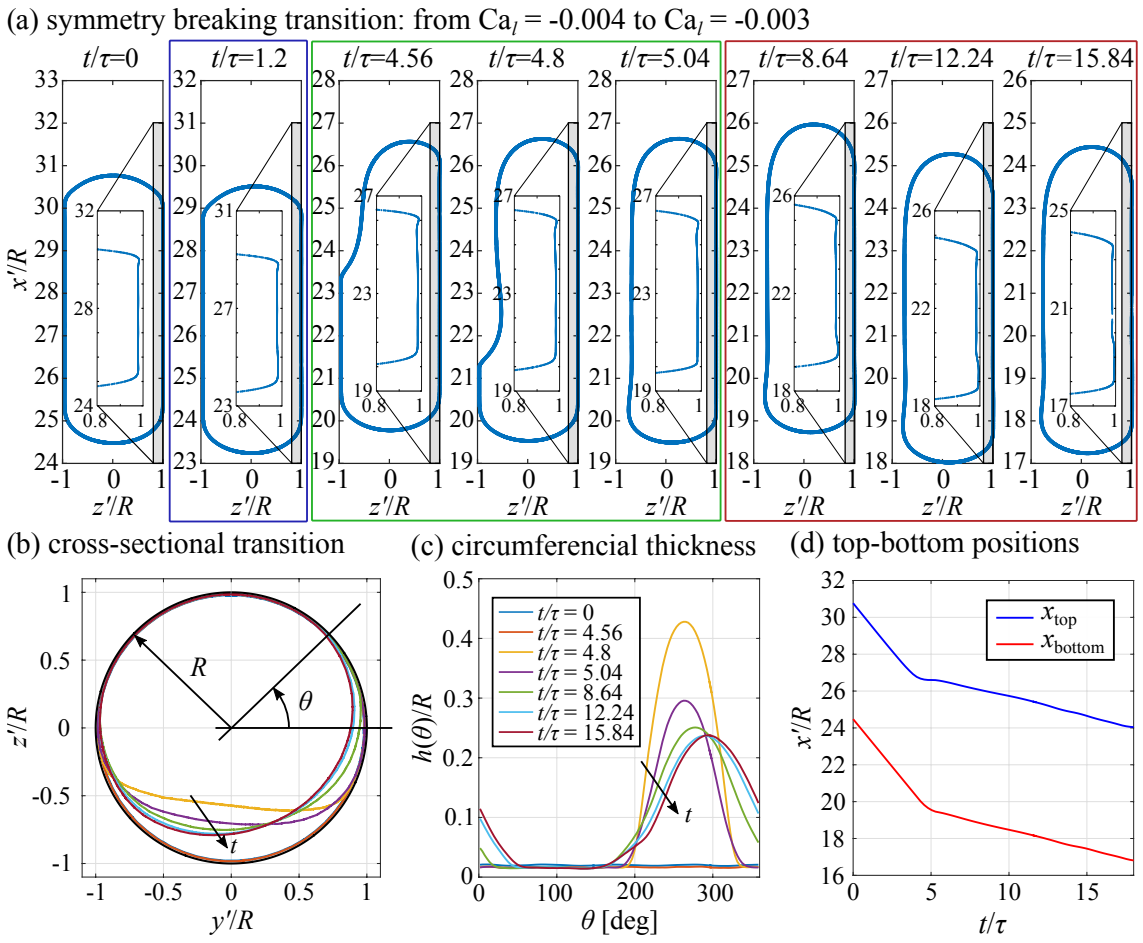

FIG. 1. Time-dependent evolution from an axisymmetric to a symmetry-breaking bubble profile starting from the left solution branch at Bo = 1.56, triggered by a change in Ca_l from $\mathrm{Ca}_l = -0.004$ to -0.003. (a) Bubble profile at different time stamps in the $y' = 0$ plane. Insets are zoomed-in views of the profiles on the right hand side. The simulation starts at $t/\tau = 0$, with the steady-state profile at $\mathrm{Ca}_l = -0.004$ as the initial condition. Three transitional stages are observed: 1) axisymmetric adjustment (blue box), 2) fast transition to asymmetry (green box), and 3) convergence to a steady-state asymmetric profile (red box). (b) Circumferential film profile measured half way between the bubble top and bottom tips, with the circumferential angle θ measured from $z' = 0$. (c) Circumferential film thickness measurements obtained from panel (b) as a function of θ. (d) The positions of the bubble top and bottom as a function of t/τ, where the bubble speed is significantly decreased after the symmetry-breaking transition.

solution, the top end of the bubble is actually shifting off-centre as time elapses. This emerges also from the bubble profile at $t/\tau = 1.2$ in Fig. 1(a), which gives way to the instability that marks the starts of stage 2.

B. Stage 2: Transition to asymmetry

At stage 2, a film thickening wave, which only spans a small portion of the bubble circumferentially, travels rapidly from the top towards the bottom of the bubble. Three successive profiles of the bubble during stage 2 are reported in Fig. 1(a), at $t/\tau = 4.56$, 4.80, 5.04, respectively.

Once the wave has travelled through the film region, the bubble sinks with an asymmetric profile circumferentially. The region where the film thickening wave passes by corresponds to a thick film, where the "nose" locates at the top end of the bubble and the "tail" at the bottom end (see Fig. 1(a) at $t/\tau = 5.04$), opposite to the orientation observed in stage 1. Meanwhile, the remaining region that is not impacted by the film thickening wave still preserves the profile and film thickness resulting from stage 1 (see the insets in Fig. 1(a) at $t/\tau = 4.56$, 4.80, 5.04), with the "nose" locating at the bottom end of the bubble and the "tail" at the top end. Therefore, stage 2 results in an asymmetric bubble profile with the thick and thin film regions showing the opposite "nose" and "tail" orientations. At the end of stage 2, the bubble sinks at a steady velocity at $\mathrm{Ca}_b = -0.00062$, which is much slower than that at stage 1.

C. Stage 3: Convergence to a steady-state asymmetric profile

During stage 3, the bubble sinks at a constant speed, with the film adjusting to a steady-state profile. Stage 2 has left the bubble with two corners along the film in the circumferential direction (see Fig. 1(b) and (c) at $t/\tau = 5.04$), and the thin film between these corners still preserves the same thickness achieved at the end of stage 1. Capillary effects thus act to round off the corners at stage 3 by generating a new film thinning wave in the thin film region. This film thinning wave travels from the bottom end of the bubble. As it travels upward, this wave thins the film even further. The simulation ceases before the wave has reached the top of the bubble, since the newly generated film becomes too thin for the

computational mesh to capture. However, based on the simulation behavior before the film dewets, where the bubble speed is not impacted by this travelling wave, the bubble dynamics is slowly converging to a steady-state asymmetric profile, with a very thin film on one side that may eventually dewet.

III. FURTHER DISCUSSION

The transition from a steady-state axisymmetric solution to an asymmetric solution is triggered by the film profile adjustment towards a new axisymmetric steady state with a thinner film. The symmetry-breaking process is composed of three distinct stages: (1) axisymmetric adjustment to a new profile, (2) rapid transition to asymmetry, and (3) slow convergence to a steady-state asymmetric profile. The resultant asymmetric bubble profile is always sinking, with opposite arrangements of the bubble "nose" and "tail" in the thick and thin film regions.

During stage 1, an axisymmetric film thinning wave propagates through the bubble body, and the transitional dynamics seems to converge to steady and axisymmetric conditions. However, the top end of the bubble slowly shifts off-centre.

Stage 2 is triggered by the off-centred top end of the bubble at stage 1, which leads to a film thickening wave that travels from the top to the bottom of the bubble rapidly. This film thickening wave sweeps through a portion of the bubble circumferentially, which leaves a thick film region, with the "nose" appearing at the top end of this region and the "tail" at the bottom end. On the other hand, in the region that is not impacted by the film thickening wave, the film thickness remains unchanged and thus preserves a thin film profile. The dynamics at stage 2 results in the asymmetric bubble profile, as well as the opposite arrangements of the "nose" and "tail" on the thick and thin film regions.

During stage 3, capillarity acts to smooth the sharp corners on the circumferential film thickness profiles. This leads to an adjustment of the profile and the generation of a new film thinning wave in the thin film region. This wave travels from the bottom end upward, but without changing the orientation of the "nose" and "tail". The film then dewets, since it becomes too thin to be captured by the computational mesh. However, based on the constant bubble speed during stage 3 and steady propagation of the film thinning wave, the bubble dynamics seems to converge to an eventual steady-state asymmetric regime.